Geothermics 140 (2026) 103712

Contents lists available at ScienceDirect

Geothermics

journal homepage: www.elsevier.com/locate/geothermics

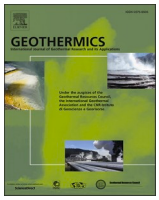

# Insights on the heterogeneity of thermal transfer in the chalk aquifer using fibre-optic distributed temperature sensing

Katerina Kyrkou [a,*], Joseph Kelly [a,b], Adam Booth [a], Fleur Loveridge [b], David Boon [c], Edward Hough [c], Lawrence Scott [d], Matthew Jackson [e], Adrian Butler [f], Daniel Perez [g], Athena Chalari [g]

[a] School of Earth & Environment, University of Leeds, Leeds LS2 9JT, UK
[b] School of Civil Engineering, University of Leeds, Leeds LS2 9JT, UK
[c] British Geological Survey, Nicker Hill, Keyworth, Nottingham NG12 5GG, UK
[d] Aquifer Energy, Main Street, Long Whatton LE12 5DF, UK
[e] Department of Earth Science and Engineering, Imperial College London, South Kensington, London SW7 2AZ, UK
[f] Department of Civil and Environmental Engineering, Imperial College London, South Kensington, London SW7 2AZ, UK
[g] Silixa, Centennial Ave, Elstree, Borehamwood WD6 3SN, UK

ARTICLE INFO

*Keywords:*
TRT
DTS
Thermal conductivity
Geothermal
Fibre optics
Chalk aquifer

ABSTRACT

The design of ground-source heat pump systems depends on reliable determination of heat transport parameters, especially the ground thermal conductivity. An effective thermal conductivity, $\lambda_{eff}$, is traditionally calculated from in-situ thermal response testing (TRT), expressed as a bulk value for the depth range being tested. However, this practice is insensitive to heterogeneous heat transport within the ground, and flowing groundwater may significantly increase $\lambda_{eff}$. To characterise high- and/or heterogeneous-flow regimes, e.g. in fractured aquifers, distributed TRT observations are advantageous. Distributed TRTs using fibre-optic distributed temperature sensing (FO-DTS) have therefore been applied at a chalk site (Berkshire, southern UK) to assess heat flow and the depth variability of effective thermal conductivity and flow conditions, within boreholes reaching up to 100 m depth. With a vertical resolution of 0.5 m, FO-DTS can isolate different thermo-hydrogeological conditions in the chalk and particularly the groundwater flow horizons. Values of $\lambda_{eff}$, measured during a 3-day TRT, vary with depth between 5 and 30 W/m K, compared to thermal conductivities of 2.3–2.9 W/m K measured on chalk core samples. Zones of enhanced $\lambda_{eff}$ correlate with highly permeable flow zones in the aquifer. However, when evaluated during a 7-day cooling phase, $\lambda_{eff}$ is reduced by between 10–60% compared to values measured during heating, highlighting the potential influence of complex convection effects and vertical flow within the open borehole. Overall, this study illustrates the value of distributed spatial assessments of thermo-hydrogeological conditions, and the necessity of combining different testing approaches to characterise heat flow in dual-porosity aquifers.

## 1. Introduction

Renewable and low carbon energy sources have been widely explored over the last few decades, leading to the development of new technologies. Shallow geothermal energy sources rank favourably in terms of environmental impacts including land use, water contamination or problems around waste. Performance in terms of technical, environmental and cost is high when applied for heating and cooling of buildings (Dincer and Acar, 2015). Shallow geothermal energy is also available everywhere, and can be extracted and stored, often by using geo-exchange technologies coupled to heat pumps, so has widespread applicability for decarbonising heating and cooling of buildings and industrial processes. These advantages, along with high system energy efficiencies, make shallow geothermal energy an increasingly attractive option, but further up-scaling, understanding and management of long-term environmental impacts is required for it to contribute significantly to reaching national and international emissions targets.

Shallow geothermal energy for heating and/or cooling buildings has

* Corresponding author at: University of Leeds, UNITED KINGDOM OF GREAT BRITAIN AND NORTHERN IRELAND.
*E-mail address:* k.kyrkou@leeds.ac.uk (K. Kyrkou).

https://doi.org/10.1016/j.geothermics.2026.103712
Received 22 August 2025; Received in revised form 10 April 2026; Accepted 29 April 2026
Available online 14 May 2026

mainly been exploited via ground source heat pump (GSHP) systems, among the highest-efficiency renewable energy systems (Ahmed et al., 2022). Heat pumps operate through a vapour-compression thermodynamic cycle (Rees, 2016), although direct use of geothermal resources can also be applicable where temperatures are high enough, and 'free cooling' can be applied when low enough. Systems can be open or closed loop, depending on whether groundwater is extracted directly for use as the heat exchange fluid, or whether an additional fluid within an installed pipe network is used for this purpose. Closed loop borehole heat exchangers (BHE) using a water anti-freeze mixture or 'brine' solution are the most common approach since they are universally applicable, low maintenance costs, and independent of the ground conditions (Rees, 2016), whereas open loop systems require the presence of an aquifer, with efficiencies influenced by reservoir conditions.

Apart from the applied thermal demand, there are several factors that govern the thermal efficiency of GSHP systems, such as the borehole heat exchanger design, its thermal properties and the ambient temperature and thermal behaviour of the surrounding strata. To effectively design a BHE or open loop borehole system, it is essential to first understand the ground's potential for heat transfer and storage. Therefore, establishing thermal conductivity and groundwater conditions is important. Laboratory tests for thermal conductivity are quick and relatively low-cost. However, there are challenges related to the high cost of coring, sample quality, representativeness because cores are small scale, meaning that test conditions might differ from in-situ field conditions (e.g., due to presence of fractures and groundwater flow; Viera et al., 2017), especially in heterogeneous bedrock. Also, multiple samples and several careful tests and a consistent method are required to ensure that the obtained results are valid and comparable to in-situ thermal conductivity values (Boon et al., 2021; Loveridge et al., 2017).

For in-situ thermal conductivity measurements, Thermal Response Tests (TRT) have been established since the 1980s (Claesson and Eskilson, 1988; Eskilson et al., 1987; Mogensen, 1983). The test involves circulating a heated fluid through the closed loop ground heat exchanger (GHE) at a constant rate of flow and heat transfer and measuring the inlet and outlet temperatures. Building on this work in the 1990s, separate teams in both the USA and Sweden developed the first mobile TRT rigs (Spitler and Gehlin, 2015).

The thermal conductivity established from conventional TRTs is a bulk value of effective thermal conductivity ($\lambda_{eff}$) for the ground, which gives no information about heterogeneity and anisotropy along the length of the borehole. Furthermore, it is characterised as *effective* thermal conductivity because groundwater flow through permeable lithologies or fractures can greatly increase the measured values when thermal transport is largely advective, rather than purely conductive.

Distributed thermal response tests (DTRTs) were developed to capture vertical variations in the thermophysical properties of the ground, thus enabling a profile of $\lambda_{eff}$ with depth to be created for the ground surrounding the borehole (Wilke et al., 2020). In this context, *distributed* refers to the measurement of temperature at intervals along the length of an entire GHE borehole during the TRT. A pioneer DTRT study demonstrated that the vertical distribution of $\lambda_{eff}$ agreed well with the known stratigraphy and groundwater flow measurements of a test location (Fujii et al., 2006).

While DTRT studies over the past two decades have successfully identified macro-scale stratigraphic layering (e.g., Fujii et al., 2006; Wilke et al., 2020), they often lack the resolution to characterize dual-porosity fractured media where thermal transport is dominated by discrete, sub-metre features. In such environments, treating the ground as a series of thick, homogeneous 'multi-layers'—the current industry standard—fails to capture the extreme localized variability that dictates actual system performance.

The recent technology of fibre-optic Distributed Temperature Sensing (FO-DTS) can be applied to DTRT experiments. FO-DTS allows the measurement of temperature along a cable using the principles of Raman backscatter, although Brillouin backscatter may also be used for strain and temperature signatures. Its advantage over other technologies, including thermistor strings that have a limit to the number of sensors, is that the spatial resolution of FO-DTS may be on the order of tens of cm, depending on factors such as cable length, laser quality, splicing configuration, and fibre dispersion (Selker et al., 2006). In general, these could be considered to provide a rapidly repeatable (in the order of seconds) high-resolution description of temperature variation, and thus $\lambda_{eff}$ and aquifer heterogeneity when applied to stratigraphic intervals with geological heterogeneity at these scales.

Since in-situ measurements of thermal conductivity at heterogeneous sites is more challenging, high-resolution measurements are valuable in the presence of fractured and/or heterogeneous materials, since these are parameters that can affect geothermal fluid circulation. Understanding ground conditions in detail is important, since heterogeneity affects not only TRT results (Loveridge et al., 2013; Signorelli et at., 2007) but also the geothermal system's design, performance and thermal interference with nearby infrastructure, especially in the presence of groundwater flow and for thermal energy storage applications. A European example of a highly heterogenous formation is the Cretaceous Chalk Group, which is commonly exploited through southern and northern England, Northern Ireland, northern France, Belgium, and Denmark for geothermal applications and groundwater supply. Despite most designs of GSHP systems assuming uniform geological conditions, recent advances in understanding of heat flow within the chalk show it to be highly heterogeneous (Jackson et al., 2012).

The chalk is a dual-porosity aquifer (Price, 1987; Price et al., 1993), composed of microporous matrix that is typically crossed by fractures (Bloomfield et al., 2003; Worthington and Foley, 2023), presenting intergranular pores in the intact material of low permeability and far higher permeability through its fracture network, thus it is characterised as a karst aquifer. Since its matrix consists of a small pore-throat size, the main pathway for flow is through its fractures (MacDonald and Allen, 2001; Price, 1987). It generally shows a rapid response over many observation wells to drawdown in one well, which can be attributed to the many interconnecting fractures and bedding planes that have been opened by dissolution (Butler et al., 2009). Overall, the style, frequency and weathering of its fractures, faults and discontinuities influence groundwater flow regimes. In terms of style, discontinuities can vary from vertical joints or joint sets, subhorizontal joints, inclined conjugate joint sets and shears, faults, fractures and disaggregation due to weathering. Fracture frequency can vary both with depth and geological setting and in general, hydrogeologists presume that the permeable zone is shallower than 50 m, which is considered as the maximum depth where joints remain open and Tertiary weathering had greatest penetration. Although fracture frequency reduces with depth, there are cases where the chalk is fractured through its whole depth range, mostly associated with fault zones and/or natural hydrofracturing (Lord et al., 2002). Finally, the weathering effect derives from the chalk's subjection to various climates since its first uplift and exposure in the Early Tertiary period. Most usually, the chemical dissolution caused by acidic meteoric water has commonly led to the creation of subvertical pipes and subterranean cave systems. In terms of heat transfer, this is dominated by flow along specific horizons, particularly along persistent permeability contrasts caused by marl seams and flint bands (Hoffmann et al., 2023).

In this context, the objective of the work presented in this paper is to demonstrate that FO-DTS closed loop TRT, when applied at higher resolution, reveals a level of thermal heterogeneity in the Chalk aquifer that contradicts traditional bulk-averaging methods and hence can help in predicting heat transfer characteristics. While most DTRT research over the last 20 years has focused on simple sedimentary layers at 1–2 m resolution, this study introduces a higher level of detail. By increasing resolution to 0.5 m, we can successfully characterize fractures and complex flow patterns in karstic dual-porosity environments.

We present the results of a DTRT using FO-DTS undertaken for the UK Natural Environment Research Council (NERC)-funded SmartRes project. The aim of the work is to gain insight into the heterogeneity of

thermal transfer and shallow geothermal energy potential of the chalk aquifer by detailed characterisation of the thermal and hydrogeological conditions. Section 2 below gives details of the site and test details. Section 3 presents the results of the traditional test data, fibre optic measurements and independent thermistors, while Section 4 discusses the implications of these results.

## 2. Site and test details

### 2.1. The trumpletts farm site

The experimental Trumpletts Farm site is in Berkshire, southern UK. The site comprises a borehole array that is used for field testing in the chalk aquifer that underlies many UK urban centres and is located on the side of a dry valley where the Seaford Chalk crops out and slopes moderately from north to south.

At this site, the hydraulic properties of the unconfined chalk aquifer have been extensively characterised as part of the Lowland Catchment Area Research (LOCAR) study (Butler et al., 2009; Parker et al., 2016). Three open-holed boreholes (PL10A, B & E) were drilled to 100 m, and three piezometer boreholes (PL10C, D & F) were drilled to 40 m, all within the 70 × 60 m site (Fig. 1). Archive core was obtained from the BGS for borehole PL10A, allowing for laboratory analysis of bedrock from intervals subject to in-situ field testing. Fig. 2 summarises the borehole log (Woods, 2003) from PL10A. The site also includes an Environment Agency abstraction well (Bottom Barn), and the elevation difference across the site between this and observation borehole PL10B is 5 m. All borehole depths and instrumentation details are summarised in Table 1.

The boreholes pass through the Seaford, Lewes Nodular, and New Pit Chalk Formations (Fig. 2).

The water table is ~20 m below ground level and has an annual fluctuation of ~7 m. The slope of the water table is in the same direction as the land surface and the difference between borehole PL10B and the abstraction well is ~0.5 m, giving a hydraulic gradient of ~0.001 (Williams et al., 2006). Furthermore, a series of tests were performed in the past, including packer tests, tracer tests, geophysical logging and dilution testing at specific horizons in boreholes PL10A and PL10B (Butler et al., 2009; Mathias et al., 2007; Williams et al., 2006). These have shown that under ambient conditions groundwater enters the boreholes at the bottom and leaves via fractures at above 56–66 m AOD. Overall permeability has also been shown to reduce with depth (Williams et al., 2006). Specifically for pumping tests in borehole PL10B, inflow was observed at 21, 27.5, 78 and 81 m AOD, and outflow at 47.5 m AOD, representing horizons of enhanced permeability probably due to fracture zones (Jackson et al., 2012).

In April 2024, a series of experiments took place to begin thermal characterisation of the site as part of the SmartRes project. These

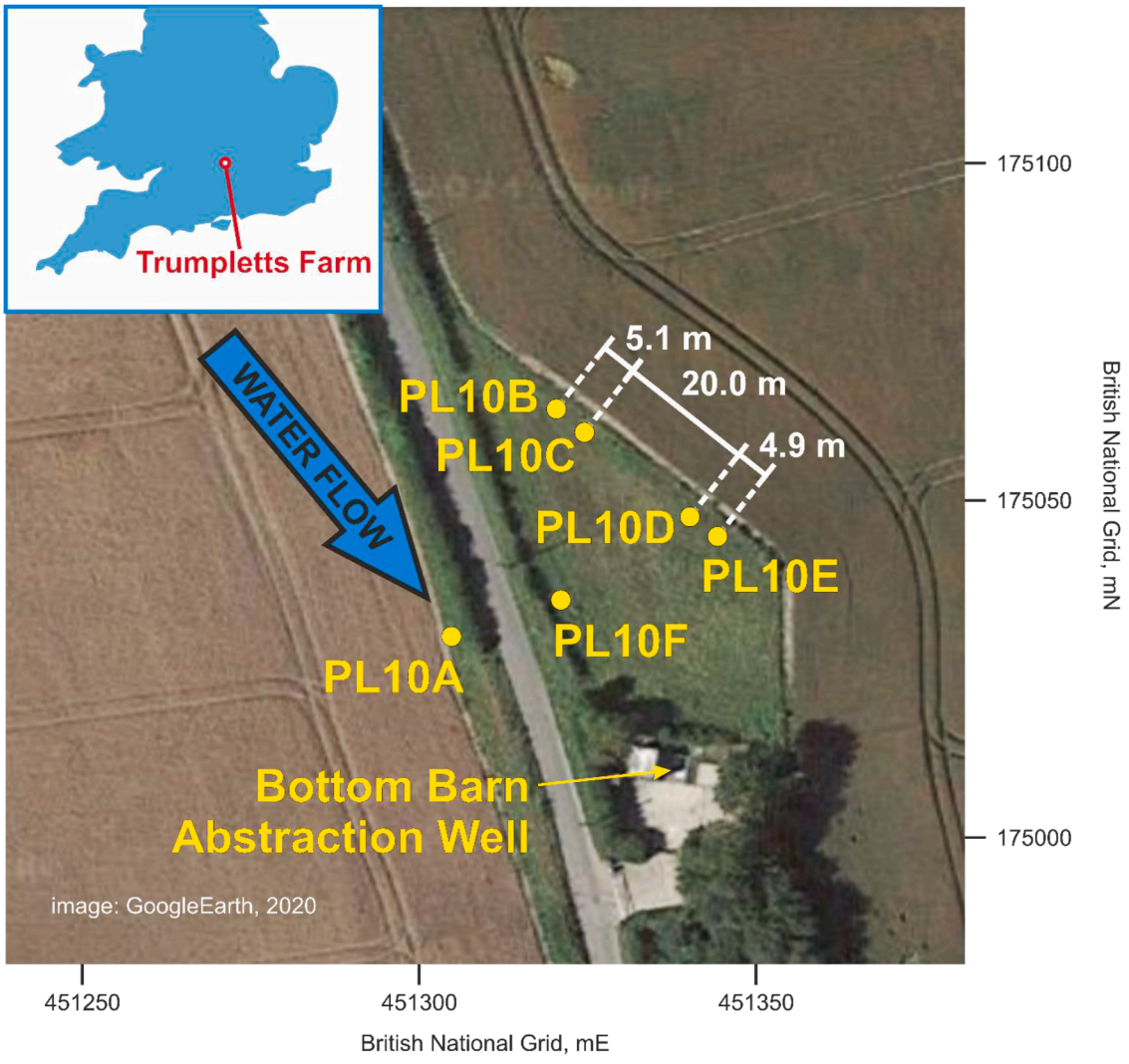


**Fig. 1.** Satellite image of the trumpletts farm site, showing the locations of the six boreholes (PL10A-F) and the bottom barn abstraction well. Google earth image includes data from maxar technologies.

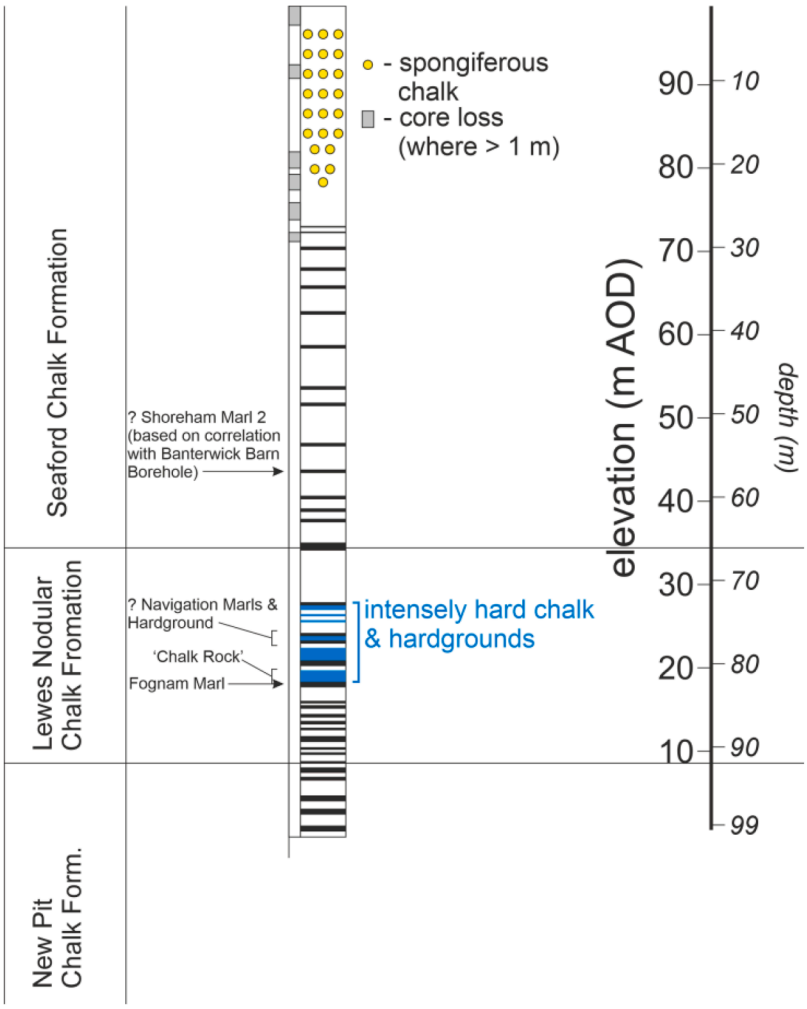


**Fig. 2.** The correlation and lithostratigraphic interpretation of borehole PL10A. Black bands in the interpretation represent fractures, with blue bands marking intensely hard chalk and hardgrounds (*adapted from* Woods, 2003. *NERC Open Access Research Archive (NORA) Available:* https://nora.nerc.ac.uk/id/eprint/527507/).

included a fibre optic distributed temperature sensing (FO-DTS) deployment during a conventional distributed thermal response test (TRT) conducted in PL10B (water-filled, 100 m deep), with additional instrumentation including FO-DTS and RST thermistor strings with 5 m node spacing installed in adjacent boreholes downstream of PL10B (Table 2). Furthermore, geophysical data have also been acquired using electrical resistivity tomography (ERT) and 20 passive seismic nodes, installed in a surface grid southwest of the boreholes for continuous monitoring of seismic energy variations. The scope of this paper is limited only to the analysis and comparison of thermal data from the FO-DTS and thermistors.

### 2.2. Test methodology

#### 2.2.1. TRT rig and test details

A single U-tube closed loop was installed in the open hole of PL10B to its full 100 m depth. The TRT was carried out according to IGSHPA/ANSI/CSA standard C448 (ANSI/CSA, 2016). The rig contained the pump for recirculating the thermal fluid (water) in the ground loop, a flowmeter to measure the flow rate and a header tank used to maintain the fluid level in the loop. An electrical heater was used for keeping the heating rate in borehole PL10B constant. The power input to the heaters and the pump was measured by a power meter and temperature sensors measured the temperature of the fluid entering and leaving the loop, the external air temperature, as well as the internal temperature of the rig. All sensors, power and flow meters were connected to a data logger for automated monitoring, and all pipework was thermally insulated to minimise any external temperature effects to the system. A schematic of a TRT rig is shown in Fig. 3.

Continuous circulation of heated fluid took place for 72 h at a constant rate of 79.5 W/m (Fig. 4), followed by 24 h of recovery, where fluid circulation continued but without heat input (Table 3). Heat was switched on at 12.00 UTC on 5th April 2024 and switched off at 12.01 UTC on 8th April 2024.

#### 2.2.2. Fibre-Optic distributed temperature sensing (DTS)

FO-DTS using Raman backscatter is based on optical time-domain reflectometry (OTDR) and was developed in the early 1980s (Hartog and Gamble, 1991). The sensing element in FO-DTS is the optical fibre itself, through which a laser is pulsed from an analyser known as an 'interrogator'. A fraction of the input laser energy is backscattered as it interacts with molecules in the fibre, with the intensity of the backscatter signal decaying exponentially over time. Knowing the velocity of light within the optical fibre, measuring the arrival time of backscattered energy allows its point of origin within the cable to be measured. The Raman component of the backscatter signal is caused by molecular vibrations that are dependent on temperature and comprises two signal peaks at different wavelengths, the Stokes and anti-Stokes. As the intensity of the Stokes peak is only weakly dependent on temperature, while the anti-Stokes is strongly dependent, the ratio between the

**Table 1**
Borehole characteristics. Borehole logs are accessible via the BGS geoIndex (https://www.bgs.ac.uk/map-viewers/geoindex-onshore/).

| Borehole ID (with BGS SOBI reference number) | Depth (m) | m AOD | Coordinates (E/N m - British National Grid) | Casing | Borehole Completion |
|---|---|---|---|---|---|
| PL10A (SU57NW/72) | 100 | 107.8 | 451,304.8/175,029.6 | 6″ Steel (150 mm) to 18 m | Open hole |
| PL10B (SU57NW/73) | 100 | 110.5 | 451,320.4/175,063.1 | 6″ Plastic (150 mm) to 20 m | Open hole / Closed loop GHE for test duration |
| PL10C (SU57NW/74) | 40.2 | 110.3 | 451,324.3/175,059.8 | 8″ Plastic (200 mm) to 3 m | Piezometers |
| PL10D (SU57NW/75) | 40 | 108.1 | 451,339.7/175,047 | 8″ Plastic (200 mm) to 3 m | Piezometers |
| PL10E (SU57NW/76) | 100 | 107.5 | 451,343.7/175,044.1 | 6″ Plastic (150 mm) to 20 m | Open hole |
| PL10F (SU57NW/77) | 40.8 | 108.1 | 451,320.5/175,035 | 8″ Plastic (200 mm) to 2.5 m | Piezometers |

two can be used to estimate temperature (Hurtig et al., 1994).

Multi-mode fibre-optic cables with single-ended measurement configuration were placed within four of the Trumpletts boreholes (PL10B-E), enclosed in a gel-filled stainless-steel capillary tube, with 4.8 mm-diameter polyamide sheathing and steel wire reinforcement. The cables were interrogated using a 4-channel Silixa XT-DTS system (Model M operating at a 1064 nm wavelength with a 2.3 ns laser pulse width), with an independent temperature measurement recorded every 0.5 m.

Each cable is interrogated individually for 1 min before cycling through to the next cable, hence the interval between temperature measurements in any one cable is 4 min. For this sampling regime and fibre length, temperature measurements are expected to be repeatable, and thus reliable, to within a ± 0.1 °C threshold. However, for unknown reasons, the interrogator occasionally skipped measurements and there are sporadic data gaps lasting up to 1 hour in the time series. A schematic diagram of the equipment used in conjunction with TRT is presented in Fig. 5.

### 2.2.3. DTS data calibration

Calibration measurements are always necessary to determine differential attenuation in DTS systems, especially for single-ended deployments of cable (i.e., where the cable termination is deep in the borehole, without a return leg for cross-validation). These can be achieved by holding a section or, ideally, two sections of optical fibre at known, constant temperatures. Typically, coils of optical fibre are placed into temperature-controlled baths inside insulated containers such that the fibre does not contact the container and experience externally influenced temperature variations. The length of the reference section of cable used for calibration, is not fixed; but longer reference fibres provide more data points, hence a more statistically robust average temperature measurement for comparison to the independent PT100 probe measurement. The difference between the temperatures is measured simultaneously by the independent probe and by the reference fibre determines the calibration offset, which is then added (with the appropriate sign) to all points of the DTS measurement. The offset should be calculated and corrected for each DTS measurement.

Since temperature is averaged over a length of fibre, the section of

**Table 2**
Timeline of testing and instrument measurement duration.

| Borehole | PL10B | | PL10C | | PL10D | | PL10E | | PL10F | |
|---|---|---|---|---|---|---|---|---|---|---|
| Date | DTS | TRT | DTS | Thermistors | DTS | Thermistors | DTS | Thermistors | DTS | Thermistors |
| 03.04.2024 | ✓ | | | | | | ✓ | | | |
| 04.04.2024 | ✓ | | ✓ | | ✓ | | ✓ | | | |
| 05.04.2024 | ✓ | Circulation and heating: ON (see Table 3) | ✓ | ✓ | ✓ | ✓ | ✓ | | | ✓ |
| 06.04.2024 | ✓ | ✓ | ✓ | ✓ | ✓ | ✓ | ✓ | | | ✓ |
| 07.04.2024 | ✓ | ✓ | ✓ | ✓ | ✓ | ✓ | ✓ | | | ✓ |
| 08.04.2024 | ✓ | Heating: OFF | ✓ | ✓ | ✓ | ✓ | ✓ | | | ✓ |
| 09.04.2024 | ✓ | Circulation: OFF | ✓ | ✓ | ✓ | ✓ | ✓ | | | ✓ |
| 10.04.2024 | ✓ * | | | ✓ | | ✓ | ✓ | | | ✓ |
| 11.04.2024 to 16.04.2024 | ✓ * | | | ✓ | | ✓ | ✓ | | ✓ | ✓ |

*FO installed full depth in all holes except after 09.04.2024, when measurements only available to 75 m within PL10B. Thermistors installed inside 30 m long, 42 mm diameter, piezometer tubes screened between 28.5-29.5 m AOD.*

*FO installed full depth in all holes except after 09.04.2024, when measurements only available to 75 m within PL10B. Thermistors installed inside 30 m long, 42 mm diameter, piezometer tubes screened between 28.5–29.5 m AOD.

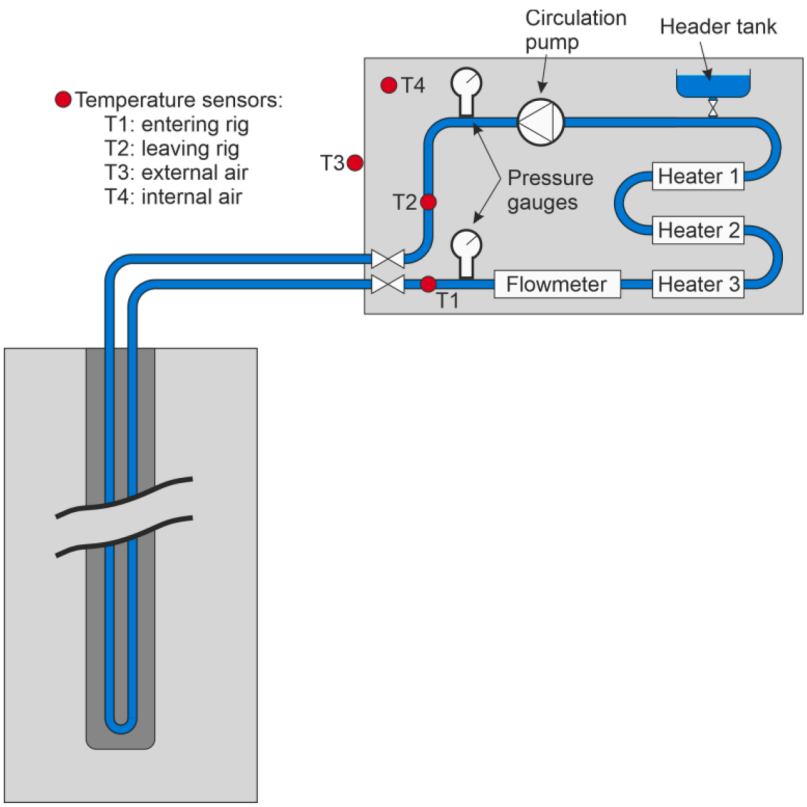


**Fig. 3.** Schematic representation of the thermal response test rig (Loveridge et al., 2013).

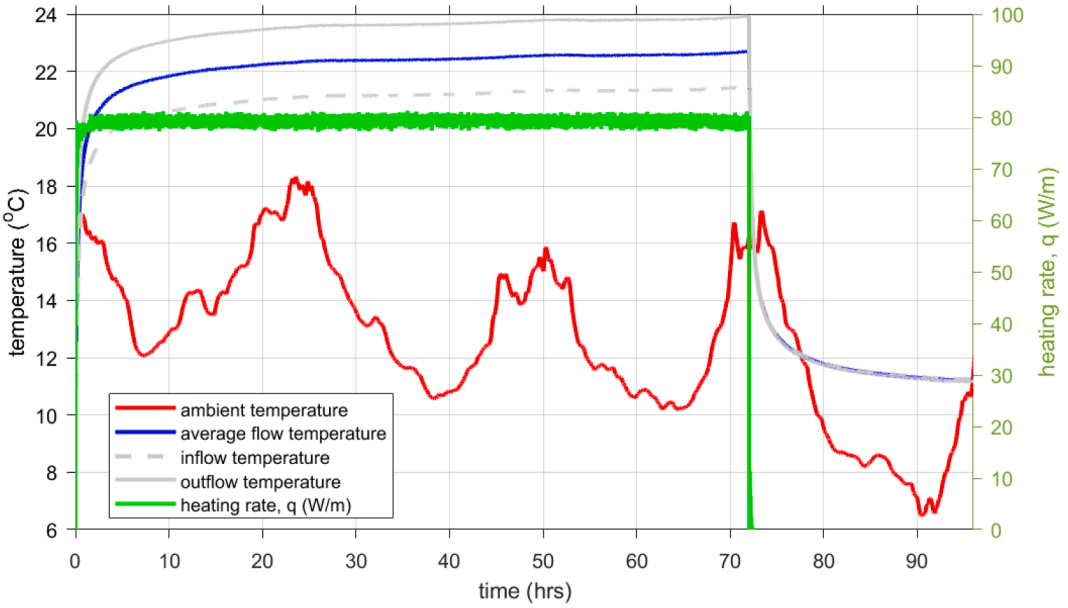


**Fig. 4.** TRT ambient and flow temperatures with power input during the 72-h heating phase, followed by a 24- h recovery phase.

fibre in the bath should be at least 10–25 m long and bath temperature should be continuously and independently monitored for reference; for the tests discussed in this paper, a standard 100 Ohm platinum RTD (Pt100) was used. Most DTS systems include automated calibration algorithms for correcting for the differential attenuation using different system configurations.

In this test though, the external offset reference fibre bath initially exhibited two issues. First, several temperature data points were significant outliers, with deviations of up to 2 °C. These anomalies were attributed to thermal inhomogeneities within the physical setup of the calibration bath. Second, the start and end points defined in the software calibration configuration were positioned too close to the physical boundaries of the fibre bath. This proximity introduced offset calibration errors, as the reference-averaged temperature was influenced by ambient temperature fluctuations in the surrounding environment. To fix the offset calibration issues, the data was reprocessed to utilise the DTS internal reference section which eliminated the artificial day-night fluctuations observed with the original suboptimal external offset

**Table 3**
Summary of the timeline for TRT .

| Date | Time (UTC) | Time since start of heating (hrs) | What was set up/removed | Comments |
|---|---|---|---|---|
| 03.04.2024 | | | ERT set up and initial cross hole survey | |
| 04–05.04.2024 | | | DTS and Thermistor Set up | |
| 05.04.2024 | 11.30 | | Fluid circulation on | DTS running since 10:25 |
| 05.04.2024 | **12.00** | 0 | TRT Heater: ON | Nominally 9 kW input (~90 W/m); Actual 79.5 W/m |
| 08.04.2024 | 12.01 | 72 | TRT Heater: OFF | |
| 09.04.2024 | 12.00 | 96 | Fluid circulation ceased | 1-day active recovery |
| 11.04.2024 | AM | | Remove GHE loop | Gap (06:37 to 15.30) in DTS during removal of GHE |
| 12.04.2024 | 10.40 | | DTS was added in PL10F | |
| 18.04.2024 | | | DTS was removed | Dataset continues until ~12.5 days post heating |
| 22.04.2024 | | | Thermistors were removed | |

calibration setup.

### 2.2.4. Thermistor installation

Negative Temperature Coefficient (NTC) Thermistor strings with nodes spaced every 5 m were suspended in the water column in the unoccupied piezometer tubes (42 mm diameter, 30 m deep) in observation boreholes PL10C, PL10D and PL10F (Table 2) to independently measure any aquifer temperature variations during the TRT. Spare nodes deployed at ground surface provided additional data on ambient temperature variations. Temperature data was collected every 2 mins between 15 April 2024 to 23 April 2024 to measure temperature change with depth independent of the FO-DTS. The thermistors were wired into a D-type (LSH20) battery-powered 40 channel RST DT2040 data logging unit and manually downloaded to a laptop computer. Logging started at 13:20 UTC (2:20pm British Summer Time) which was 18 min after the switch on of the heating elements in the TRT rig. Note that thermistor cables were not inserted into the deeper 90 mm piezo tubes or the main TRT well (PL10B), or PL10E, to avoid concerns about the cables of different monitoring systems becoming entangled during retrieval. However, thermistor strings had been deployed temporarily between 40–100 m deep in boreholes (PL10B & E) between 26 Sept and 11 Oct 2023, to record late summer/early autumn baseline equilibrium temperatures with a bottom hole temperature of 11.1 °C observed at 10.5 °C between 40–50 m down. Slight temperature variations (dropping to 9.9 °C) were observed between 50–60 m and 70 m depth intervals in the monitoring period, suggesting periodic influx of cooler water.

### 2.2.5. Thermal conductivity calculations

Assuming an infinite line heat source with a constant heat injection rate (q) per unit depth in the borehole, the effective thermal conductivity ($\lambda_{eff}$) is determined from the gradient of the graph of fluid temperature change against the natural logarithm of time according to Eq. (1). The fluid's average temperature change ($\Delta T_f$) is calculated in relation to the heat transfer within the borehole as

$$\Delta T_f = qR_b + \frac{q}{4\,\pi\,\lambda_{eff}}\left[\ln\left(\frac{4\,\alpha\,t}{r_b{}^2}\right) - \gamma\right] \quad (1)$$

The first term in Eq. (1) describes the temperature change between the fluid and the borehole's edge, calculated based on the borehole's thermal resistance ($R_b$), and the second term describes the temperature change at the borehole's edge (radial coordinate, $r_b$). In this equation, α represents ground's thermal diffusivity, γ is Euler's constant (γ =0,5772), q is the heat flux per unit depth. On this basis, the gradient of a temperature change vs. ln (time) plot can be used to determine the effective thermal conductivity.

This approach can be followed to calculate the effective thermal conductivity of the ground using the fluid temperature data. However, the gradient of ΔT vs ln(t) can also be used to determine to $\lambda_{eff}$ for any depth in the DTS dataset. In all cases, measurements made during the first 5 h of heating were neglected to ensure that any transient effects in the borehole could be neglected, and also that the straight-line approach in Eq. (1), which is a mathematical simplification, remains valid. The 5-hour period is an empirical value derived from thermal response tests of similar design.

Effective thermal conductivity was also calculated for the recovery phase, with analysis commencing 5.8 h after the 72 h of heating. A longer period of omitted data was chosen to allow gradient calculations to span a period over which temperature changes were more linear, and therefore valid for the simplified straight-line fit. A marked dip in the

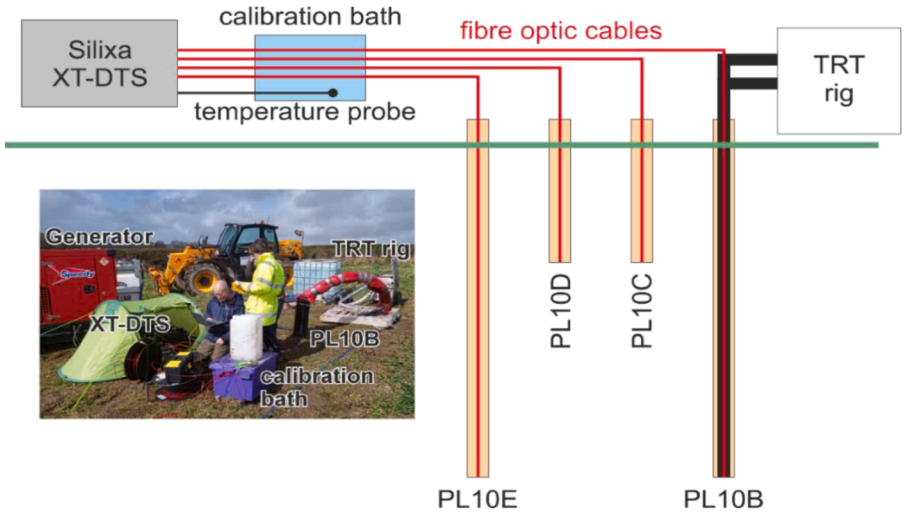


**Fig. 5.** Schematic diagram of TRT and DTS operations at trumpletts farm, with field photograph inset.

slope of the recovery phase DTS data is interpreted as resulting from an overnight drop in ambient temperature affecting the calibration, thus calculation spanning this period was avoided. In the recovery phase, the approach is similar, except that Eq. (1) becomes:

$$\Delta T_f = \frac{q}{4\,\pi\,\lambda_{eff}}\left[\ln\left(\frac{t}{t'}\right)\right] \quad (2)$$

where t' is the time elapsed since the heater was switched off. Because the borehole thermal resistance does not feature in Eq. (2), thermal conductivity derived from recovery data can be viewed as more reliable (Raymond et al., 2011).

All key timeline details for TRT and DTS are summarised in Table 3.

## 3. Test results

### 3.1. Undisturbed ground temperature

Before heat injection was started, the ambient temperature in borehole PL10B was measured (Fig. 6a), as well as the fluid temperature, being approximately 12 °C.

Furthermore, available DTS data were compared with the temperature measured by thermistors in borehole PL10C, consistent to ~ 0.5 °C (Fig. 6b). This discrepancy could be attributed to the effect of piezometer pipes in the borehole, since the DTS and thermistors are installed in different pipes with difference response zones. The two instruments are also calibrated differently, the DTS via an internal sensor, and thermistor strings being factory calibrated. Nonetheless, the 0.1 °C error for DTS results indicates the repeatability of measurements.

### 3.2. TRT fluid data

As listed in Table 3, water was circulated within borehole PL10B and heated at an approximately constant rate ($q$ in Eq. (1)) of 79.5 W/m (Fig. 4). The ambient air temperature during the test can been seen to vary between day and night, and day to day (Fig. 4). Because it is not possible to perfectly insulate all surface pipework and furthermore, this particular test includes a section of pipe within the air within the borehole above the water table (0–20 m depth), this does result in some minor variations in heat transferred to the ground water and ground during the test.

The fluid data can be used to make a traditional estimation of effective thermal conductivity for both heating (5–72 hrs) and recovery (77- 96 hrs) phases using Eqs. (1) and (2) respectively. These are plotted as a function of time, along with the air ambient temperature, are shown in Fig. 7. Calculation of the effective thermal conductivity was established using a progressively lengthening window with a starting time fixed at 5 h, and an end point increasing up to 72 h. Effective thermal conductivity is observed to be unrealistically high (>5 W/mK) and to increase with time, which is due to groundwater flow. The implied conductivity is also different during the heating and recovery phases. Both these phenomena are discussed in more detail in Section 4.2. Because of the small heat transfer fluctuations, a small (< 0.5 W/mK) influence of ambient air temperature is observed in the heating phase estimate, evident from the minor undulations in the response, which are anticorrelated with the ambient air temperature.

### 3.3. DTS data

DTS data were analysed to illustrate temperature variations with depth and time for borehole PL10B (Fig. 8), showing that during the heating phase, zones of lower temperature are observed to correlate with known groundwater flow zones based on available pumping test data in boreholes PL10A and PL10B.

Under the ambient flow regime, heat injection in borehole PL10B is expected to circulate through the chalk's fractures and potentially affect the temperatures in adjacent boreholes PL10C, PL10D and PL10E based on the local groundwater flow direction. The time that temperature change is observed in the adjacent boreholes is called thermal breakthrough. However, even though the chalk in this area presents a dense fracture network, no breakthrough (i.e., deviation from the baseline temperature state) was observed within the 72-hour heating period or any time after it in PL10C which is the closest monitoring borehole (Fig. 9). Thermal breakthrough was also not evident in PL10C thermistor

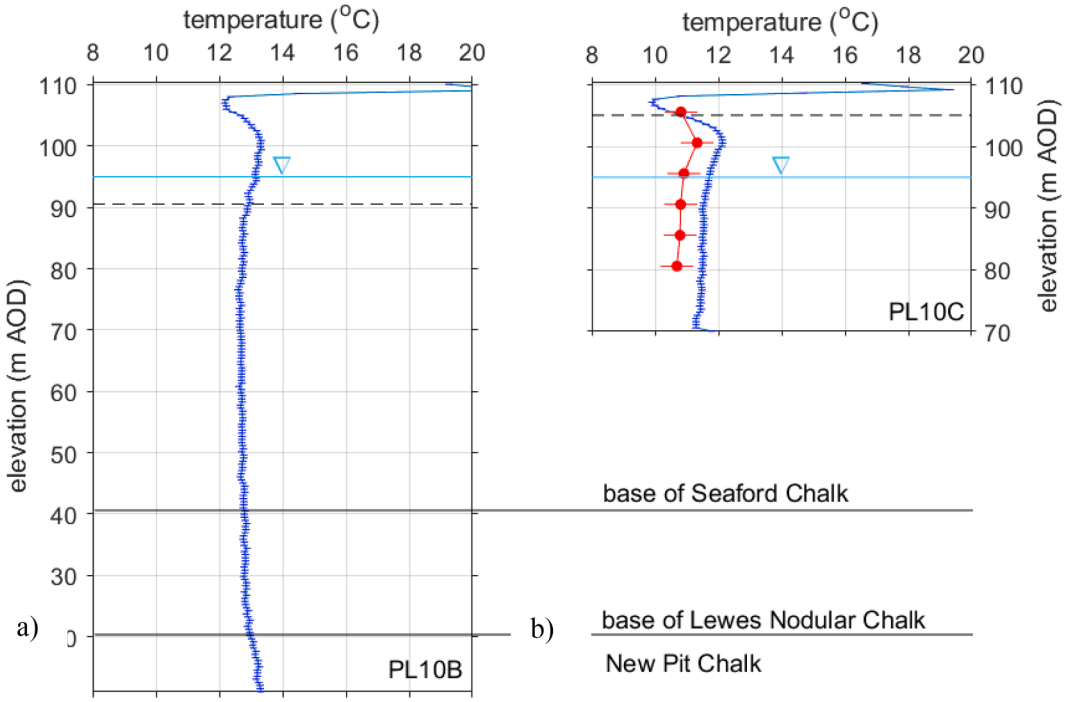


**Fig. 6.** Undisturbed ground temperatures from DTS (blue) and thermistors (red) for boreholes (a) PL10B and (b) PL10C. Casing elevations are shown by the black dashed line (90.51 and 105.05 m AOD in PL10B and PL10C, respectively). The water table (blue horizontal line, symbol ▽) at the time of the TRT was ~ 95 m AOD.

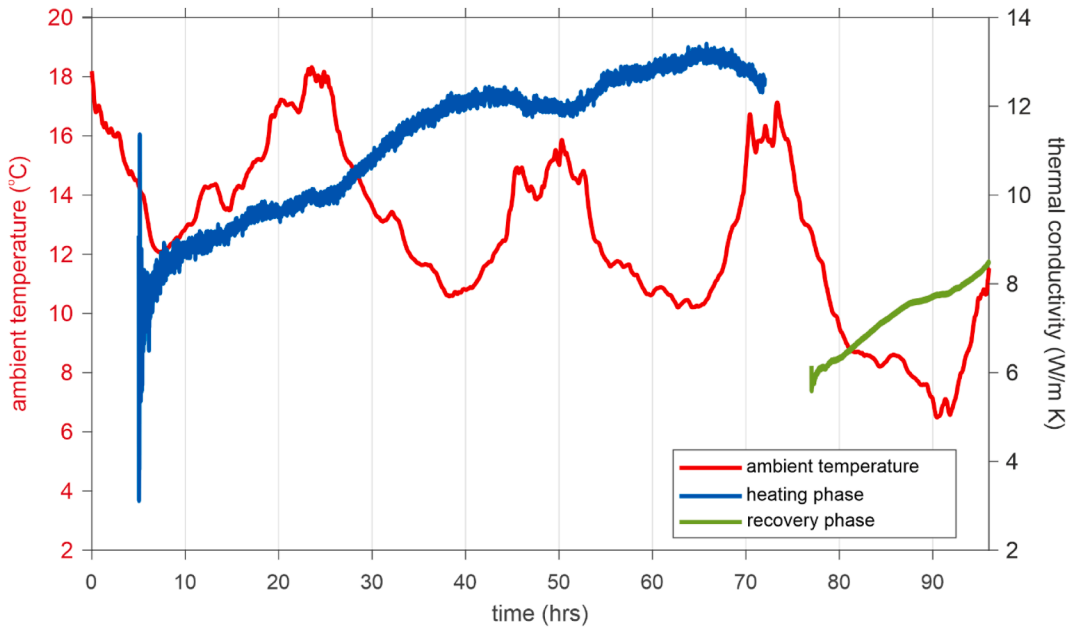


**Fig. 7.** Effective thermal conductivities derived in PL10B from fluid temperatures during TRT heating (blue) and recovery (green) phases, and ambient air temperature (red).

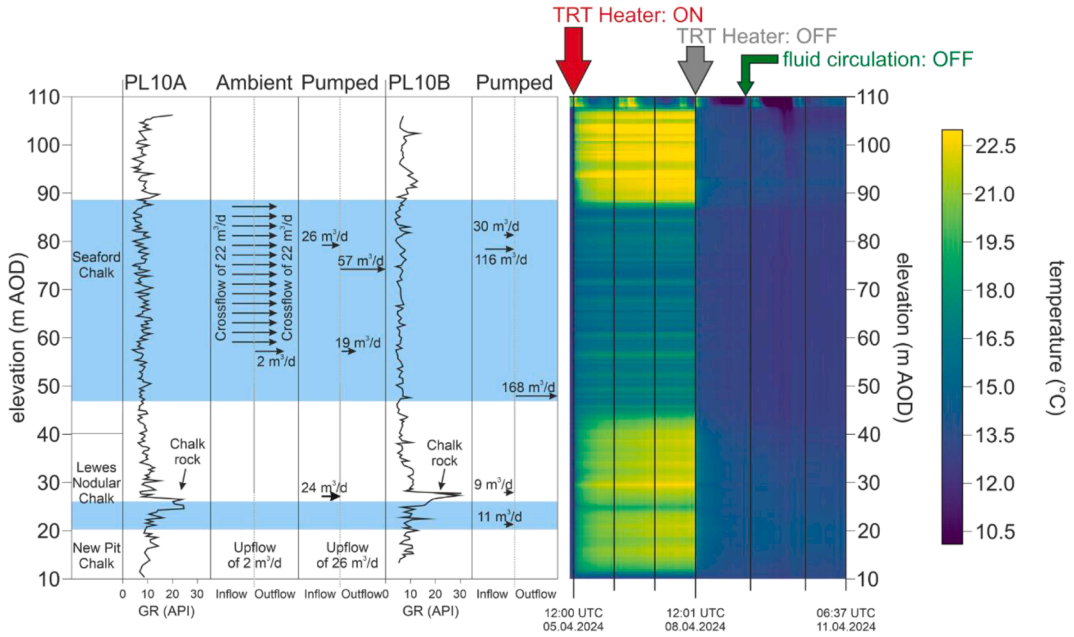


**Fig. 8.** Correlation of the waterflow zones in boreholes PL10A and PL10B (left, adapted from Jackson et al., 2012), and a thermal map showing DTS temperature-elevation variations before, during heating and in the recovery phase of the TRT in borehole PL10B.

data.

The very near surface (>108 m AOD) temperature variations observed in Fig. 8 are unrelated to the heat injection and are attributed to the influence of ambient air temperature in the unsaturated, open section of the borehole above the water table.

DTS data after the TRT heater was turned on were used to calculate thermal conductivity along the length of the fibre optic cable in PL10B. For comparison with the thermal conductivity calculated from the fluid data, 5 depths (76.5 m, 55.5 m, 35.5 m, 26.5 m and 19.5 m AOD) in the borehole were selected in the different chalk formations. Effective thermal conductivities are shown as a function of time in Fig. 10 and 11 for the heat injection and recovery phases, respectively.

Table 4 shows the mean effective thermal conductivity measured for the five representative elevations, through both heating and recovery phases (spanning 5–72 hrs and 84.9–87.7 hrs after the start of the TRT, respectively) and also the traditional depth average effective thermal conductivity for the entire borehole calculated using the fluid data over the same time windows. At the same site, saturated thermal conductivity has also been measured on core samples obtained from borehole PL10A using a Modified Transient Plane Source (MTPS) method (Nair, 2023).

The average thermal conductivity measured for laboratory samples, 2.7 W/m K, is significantly lower than the effective values determined from either the FO-DTS or the fluid temperatures. Furthermore, values recorded from FO-DTS show much more variability with depth, both

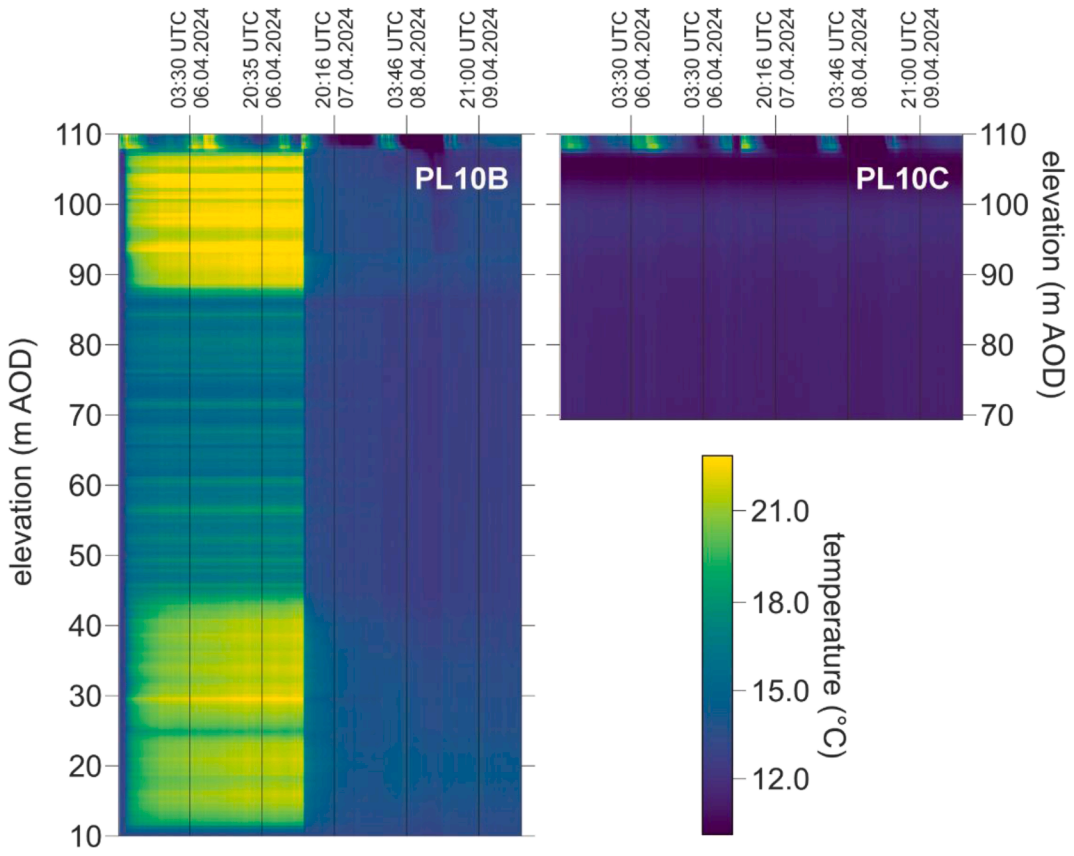


**Fig. 9.** Temperature variations over depth and through time plots for boreholes PL10B and PL10C from the TRT heating phase. The consistency of temperature in PL10C implies no thermal breakthrough in this borehole.

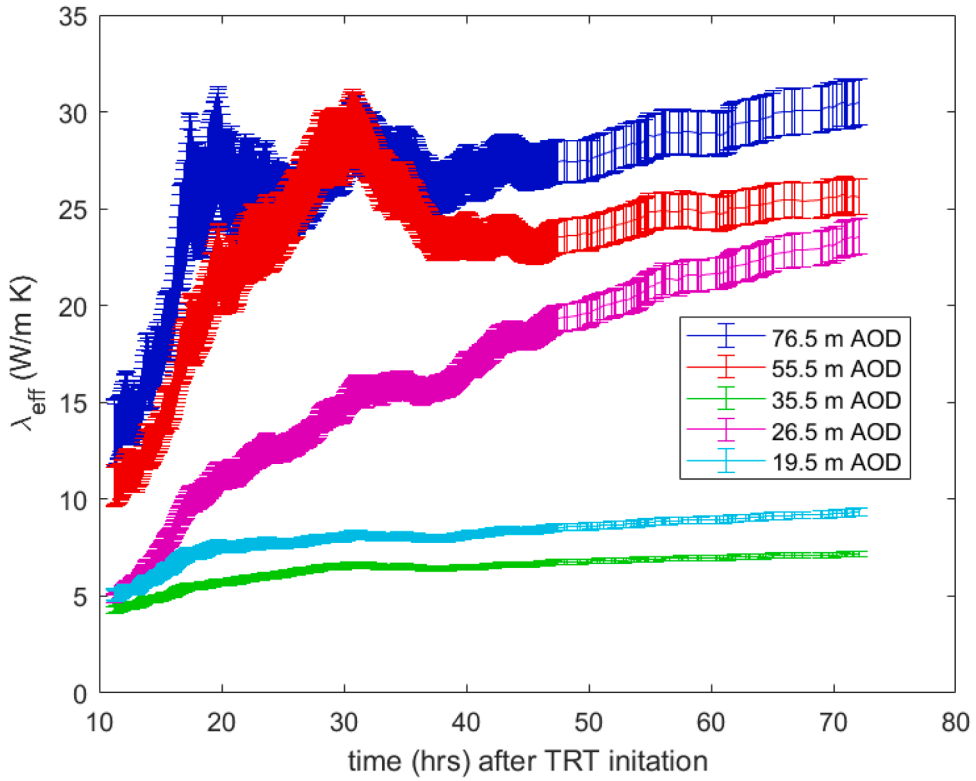


**Fig. 10.** Variation in $\lambda_{eff}$ with time, evaluated from FO-DTS data during the TRT heating phase for representative elevations. Error bars correspond to the standard error in straight-line fitting through the temperature plots, combined with the standard deviation of power input (q) through time.

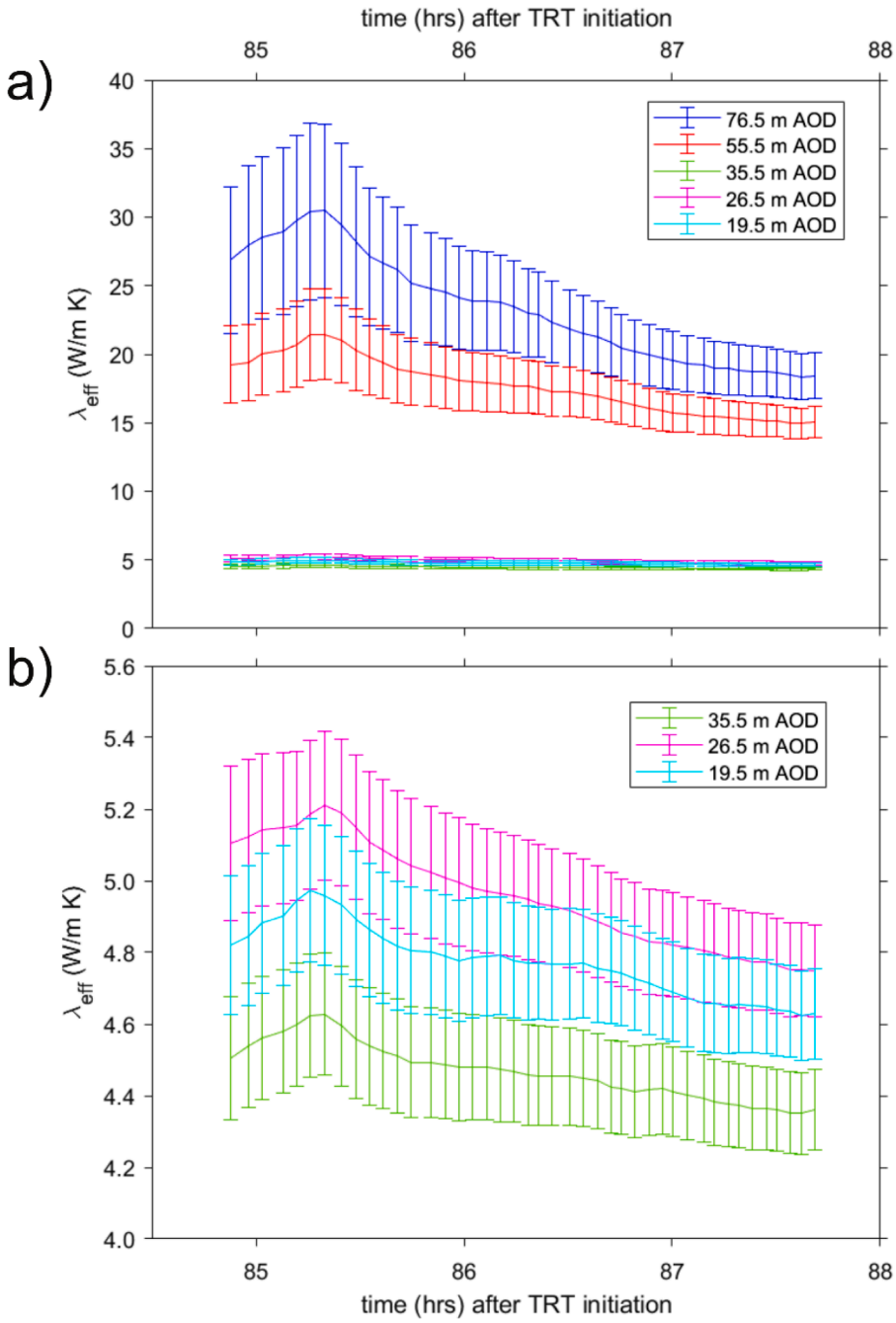


**Fig. 11.** a) Variation in $\lambda_{eff}$ with time, evaluated during the TRT recovery phase, for the elevations shown in Fig. 10. b) Enlarged view, for elevations of 35.5 m, 26.5 m and 19.5 m AOD.

compared with the depth averaged effective thermal conductivity and also the laboratory data. This is especially so for the uppermost 55 m of the Seaford Chalk, which likely relates to horizontal advection-driven groundwater flow affecting that zone. The variation in average thermal conductivity for all depths of the FO-DTS, through both heating and recovery phases, is shown in Fig. 12.

It should be noted that around 2 m have been trimmed from the top and bottom of the plotted data. This is due to end effects at the bottom of the borehole not being properly modelled by the infinite line source method, as well as ambient temperature influence at the top, which lead to very erratic values in these regions.

### 3.4. NTC thermistors

The measured average aquifer temperature between 15 m and 30 m (below the water table and below the zone of seasonal interaction) between 05.04.2024 and 23.05.2024 was 10.75 °C. The equilibrium bottom hole temperature 100 m below ground level measured between 25.09.2023 and 11.10.2023 was 11.1 °C, increasing from 10.6 °C at 40 m depth. These temperatures are the same as the September-October 2023 baseline values. This was independently verified using a Solinst 106 TLC Meter and British Geological Survey downhole logging in May 2023. There was little variation except within a zone between 50–60 m where static well water temperatures fluctuated between 10.0 and 10.5 °C, suggesting some recharge flow coming into this zone.

The thermistor data from the observation well PL10C, located ~8 m

**Table 4**
Comparison of mean and standard deviation for $\lambda_{eff}$ observed in Figs. 10 and 11, and laboratory tests, for selected depths. Laboratory measurements use the MTPS method for water-saturated core plug samples taken from borehole PL10A (Nair, 2023).

| TRT Results from PL10B | | | Laboratory data (MTPS method) from PL10A core | |
|---|---|---|---|---|
| Elevation (m AOD) | Mean $\lambda_{eff}$ with standard deviation | | Chalk formation * Intrinsic λ (min-max) | |
| | *Heating phase* | *Recovery phase* | | |
| Depth averaged from fluid data | 11.3 ± 1.5 | 7.6 ± 0.7 | | |
| 76.5 | 25.7 ± 3.9 | 23.1 ± 3.9 | Upper Chalk (Seaford Chalk) | 2.3–2.8 |
| 55.5 | 22.8 ± 4.5 | 17.6 ± 2 | | |
| 35.5 | 6.2 ± 0.7 | 4.5 ± 0.1 | | |
| 26.5 | 14.6 ± 4.5 | 4.9 ± 0.1 | | |
| 19.5 | 7.8 ± 0.9 | 4.8 ± 0.1 | Middle Chalk (Lewes Nodular Chalk) | 2.4–2.9 |
| | | | Lower Chalk (New Pit Chalk) | 2.5–2.6 |

* Seaford Chalk conductivity values were measured at 34 m depth; Lewes Nodular Chalk values were taken at 91 m depth; New Pit Chalk values were measured at the bottom of the borehole.

from PL10B, did not show clear thermal breakthrough during the 72-hour heating and 24-hour recovery period. A minor increase of 0.02 °C was observed at 29.66 m depth in PL10C, some 90 h after the initiation of heating and the increase rose to 0.06 °C after around 333 h, but this change is close to instrumental stability (0.01 °C) thus is deemed inconclusive.

## 4. Discussion

Fig. 12 illustrates the significant heterogeneity in the thermo-hydrogeological conditions in the Chalk aquifer at this site that can only be detected by high resolution spatial measurements such as FO-DTS. The following sections explore in more detail the value of the FO-DTS measurements, and the inferences that can be made about the heat transfer regime at the site, and the resulting implications for shallow geothermal assessment and adoption.

### 4.1. The value of FO-DTS

The FO-DTS results show starkly the changes between the groundwater no-flow zones above the water table, the high flow zones in the Seaford Chalk, and even a spike of reduced temperature change related to expected flow in the Chalk Rock at greater depth (Fig. 8). In this field experiment, the spatial resolution of the FO-DTS was set to 0.5 m to balance vertical resolution and the signal to noise ratio in measurements. At this level of granularity, adjacent measurement points sometimes showed differences in temperature of up to 3 °C and derived thermal conductivity is shown to vary up to 15 W/mK in less than a metre for the heating phase data, and up to 9 W/mK in the recovery phase. It is important to assess whether these rapid changes in properties could be representative of in-situ spatial variability or whether the technique does not have the repeatability or reliability to capture this type of detail.

With the experimental settings applied, it is expected that fibre-optic temperature measurements achieve an accuracy of ±0.03 °C and repeatability of ±0.1 °C. These capabilities give confidence that the variations measured with depth are indeed representative of in-situ conditions. In addition, recent application of FO-DTS and FO-distributed strain sensing (FO-DSS) for assessing the integrity of piled

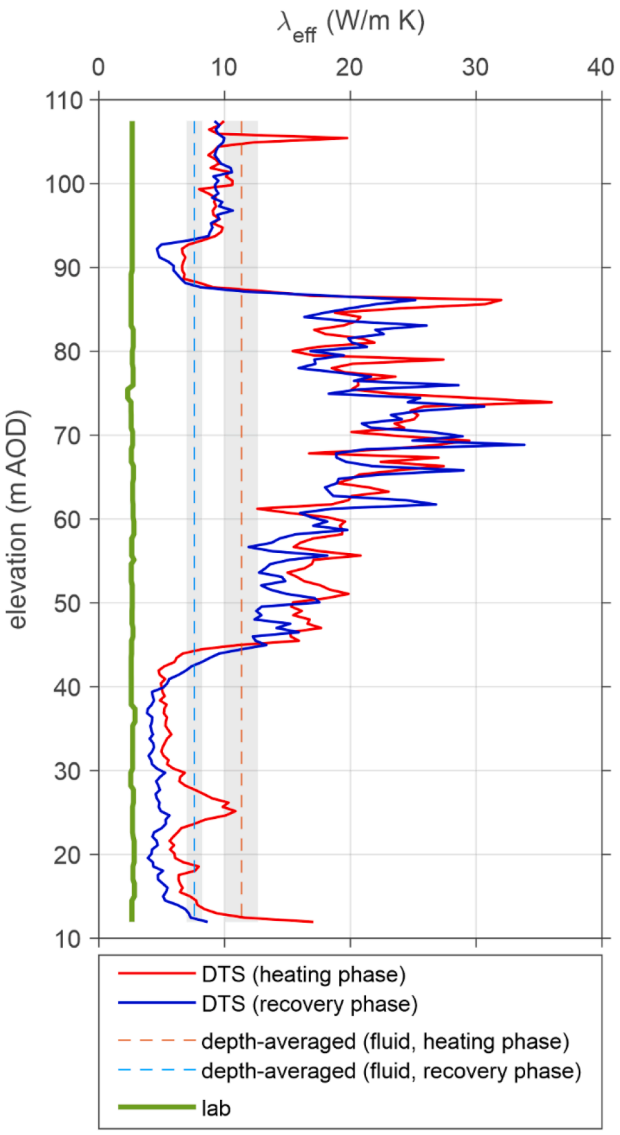


**Fig. 12.** FO-DTS and fluid derived thermal conductivity results from heating and recovery phases, compared to the laboratory values obtained across all depths in borehole PL10B. TRT interpretation time windows of 5–72 hrs and 77.8–87.7 hrs for heat injection and recovery respectively.

foundations have shown similarly highly depth variable results. These were traced to changes in the pile diameter with depth caused by the combination of the construction process and natural changes in the surrounding stratigraphy, that included the Chalk at the base of the pile (Soga, 2025). In particular, the same pattern of highly wavey spatial variability was observed in four different DO-DSS cables as well as the temperature measurements. In this case the variability was at a larger scale than the measurement interval (10 cm), giving weight to the argument that the results were representative. This experience gives further confidence that the sub-metre level changes in thermo-hydrogeological behaviour of the Chalk at Trumpletts Farm is a reflection of natural geological heterogeneity and not the measurement process. This is further supported by the presence of thin hard nodular bands and marls, also fracture horizons identified in the core logging (Fig. 2) and from televiewer observations, plus observed concentrated water inflow locations (Fig. 8 and Butler et al., 2009).

The presence of the highly variable thermal response, as captured by the FO-DTS, suggest that a standalone conventional TRT is most probably not an appropriate investigation method in such cases. For closed loop GHE, their design is typically based on single average value of

thermal conductivity. However, taking the fluid-derived effective thermal conductivity from this test without understanding the context of the measurement could be very misleading. First it must be questioned how much groundwater influence can be relied upon, and second it is known that stratified ground does affect system thermal behaviour (e.g. Signorelli et al., 2007). For open loop systems, understanding the relative importance of the different parts of the aquifer is even more important since drilling and abstraction can be targeted to the most appropriate aquifer zones. A pumping test alone in PL10B would not have identified the stratification of the flow horizons. Therefore, a DTRT can be recommended for both applications in known heterogeneous formations. The use of 5 m spaced thermistors at this site showed their spatial resolution is not necessarily sufficient to identify the highly heterogeneous features present, such as some of the discretely fractured zones in the chalk, highlighting the advantage of FO-DTS in these cases.

### 4.2. Derived thermal conductivity values

The effective thermal conductivity determined from the classical thermal response test data (i.e., the circulating fluid) is significantly higher what would be expected for the rock materials at the site. This is confirmed by the laboratory thermal conductivity testing which has a mean of 2.7 W/m K compared with 11.3 ± 1.5 W/m K from heat injection and 7.6 ± 0.7 W/m K from recovery. Even the recovery value, which could be taken to be more reliable (Raymond et al., 2011), is significantly elevated. Taken together with the value which rise with inclusion of larger data assessment windows, these results strongly suggest the presence of major natural groundwater flow. The FO-DTS results (Fig. 8) allow correlation of this flow with key fracture flow horizons already identified.

### 4.3. The differences between heating, recovery and laboratory testing

The difference between the heating and recovery thermal conductivities derived from the fluid data can be caused by several factors. The difference in heat transfer rates in different parts of the GHE, combined with any positive geothermal gradient, can mean that TRT results take proportionally greater influence of the upper part of the borehole during heat injection and the lower part in recovery (Loveridge et al., 2013). This alone could explain some of the results given the much higher effective conductivities and therefore flow rates in the Seaford Chalk.

The difference between the heating and recovery thermal conductivities derived from the FO-DTS are less significant in the Seaford Chalk than the lower part of the borehole. This suggests that different processes are important here, and it is known that up-flows are present from the base of the hole (Butler et al., 2009; Jackson et al., 2012, also Fig. 8). This within-hole processes, as well as any free convection within the water-filled hole, would influence the thermal resistance of the borehole. This term does not feature in the recovery analysis and therefore may more greatly influence the heat injection derived values.

Previous flow characterisation in PL10B (Butler et al., 2009; Jackson et al., 2012) also suggests very little flow in the lower part of the hole in the Lewes Nodular Chalk. The difference between the laboratory data and the FO-DTS data here is still significant, with the DTRT results approximately twice that of the laboratory data. This could contradict the flow testing, suggesting that there is still some potential matrix flow or minor fracture driven flow in the dual porosity media at this location. However, the potential for upward flow and any buoyancy-driven flow within the hole, influences the thermal response and makes this interpretation uncertain. For a more traditional DTRT in a grouted closed loop GHE, these differences may not have been so apparent.

### 4.4. Absence of thermal breakthrough

The results obtained by FO-DTS in boreholes PL10B and PL10C of the heating phase showed no measurable thermal breakthrough in the nearest borehole to the TRT (i.e., PL10C - Fig. 9). The same is the case for the thermistors installed in these holes though the results were inconclusive due to measurement resolution limitations of the equipment being close to the magnitude of thermal changes and the monitoring period being too short to capture the return to ambient conditions. Numerical modelling of this site with a series of simulations was also undertaken by Bahlali et al. (2025). This explored various scenarios; variable permeability and dispersivity, as well as thermal equilibrium and non-equilibrium between groundwater flow both in the chalk fractures and the matrix (Bahlali et al., 2025). In high-dispersivity and/or thermal equilibrium scenarios, the thermal plume migration was broader but led to lower temperature anomalies. This is one reason why thermal breakthrough was not detected on this site with such significant natural groundwater movement. On the other hand, an assumption of non-local thermal equilibrium can potentially mean measurable thermal plumes progress over much more substantial distances. However, in this case, unless the monitoring point directly intersects the discrete flow path in a fracture, the plume may not be detected by monitoring points. These two end member behaviours cannot be separated from the data obtained in this experiment, and reflect the challenge in how to investigate, characterise and monitor high natural flow aquifers for geothermal utilisation. These conditions also illustrate how sites like these may prove excellent for thermal heat extraction, but present challenges for energy storage. Monitoring of these systems may also be challenging where groundwater flows are high and focussed in discrete fracture zones.

### 4.5. Engineering implications: exploiting high effective-conductivity horizons

The identification of sub-metre horizons with effective thermal conductivities exceeding 15 W/m K presents an opportunity for optimized geo-exchange design. In such highly advective zones, standard closed-loop Borehole Heat Exchangers (BHEs) may be limited by the thermal resistance of the grout and pipe material rather than the ground itself.

To maximize heat collection in these 'thermal hotspots,' several alternative approaches could be considered:

1. Optimizing the borehole length, so that additional drilling expense beyond the dominate advective zones is not incurred, increasing the heat transfer available per drilled metre and reducing drilling cost.
2. Optimizing the closed loop borehole heat exchanger design. This could include consideration of coaxial heat exchangers, higher thermal conductivity grout or selective backfilling with high permeability granular materials to exploit the in-situ flow.
3. Switching to open loop: such high flow horizons may make open-loop applications more cost-effective and use of the FO-DTS data allows for 'precision screening' of the borehole. By targeting only the discrete high-flow fractures identified, operators can maximize abstraction efficiency while minimizing the risk of drawing in poor-quality water from non-productive matrix zones.

### 4.6. Recommended options for DTRT

As discussed above, use of DTRT brings advantages in terms of better conceptual understanding of the ground conditions, more appropriate design parameters, and opportunities for enhanced design. However, the disadvantage of FO-DTS for DTRT in routine practice is that the test would come with added expense. The use of DTRT does not need to change the duration of the test, but it does require additional instrumentation and monitoring. The most cost-effective way to achieve this is with thermistor strings, but these do not give such high resolution as FO-DTS as discussed above. While fibre optic cable is relatively inexpensive (order of magnitude £100 s for a typical shallow borehole), the capital cost of an interrogator to capture the data is two orders of magnitude

greater (£10,000 s). The most cost-effective way to gain distributed measurements would be to disconnect the TRT rig post heat injection and lower a re-usable thermistor string into the pipe loop. This would not allow calculation of thermal conductivities, but would allow identification of horizons of enhanced thermal properties, either due to geological variability, stratification or flow horizons. Ultimately the choice between these options and also a traditional TRT will likely follow site desk study and initial ground model development. This should highlight whether there is the potential for significant heterogeneities that may impact diffusive or advective heat flow, and the investigation technique should then be chosen to reflect both the ground conditions and the nature and size of the planned shallow geothermal application.

## 5. Conclusions

Understanding the thermal properties of the ground is essential for the design of ground source heat pump systems for space heating and cooling. Among these properties, thermal conductivity and groundwater conditions are considered most important in underpinning the ground's potential as a heat source and store. Measurement and characterisation of this thermo-hydrogeological performance through appropriate in-situ testing is critical for ensuring sustainable and long-term management of the geothermal resources, especially in large-scale projects, such as hospitals or school buildings.

One of the most widely used in situ tests for closed loop GHE characterisation is the thermal response test (TRT). Taken together with new technologies such as fibre-optic DTS systems, distributed TRT (DTRT) can provide a detailed insight into even complex and heterogeneous geothermal aquifers, such as the chalk, for both closed and open loop applications.

This paper presented the results of field tests performed in the UK, including fibre optic (FO) DTRT, aimed to assess the thermal conductivity and groundwater conditions of the chalk aquifer. Data were collected through a period of 14 days where the circulating fluid was heated for 3 days, followed by a 24-hours recovery phase and ongoing monitoring. The following are the key findings of the work:

- FO-DTS in TRT proved to be a valuable tool in identifying even thin beds and features within the chalk, especially where groundwater movement was significant. The FO-DTS results showed clearly showed the different hydrogeological regimes in different parts of the Chalk stratigraphy.
- At this site, the dominance of fracture flow and speed of equivalent water velocity means it is difficult to track the injected heat to downstream boreholes. This is a significant consideration for characterisation and design of monitoring strategies of future applications of shallow geothermal in these conditions.
- Natural upflow and potentially also free convection effects within the borehole may have impacted the thermal conductivity values derived from the DTRT. This is potentially more significant during the heating phase. Generally, having data describing the recovery stage of a TRT too can be beneficial for deriving more reliable results, but does result in additional costs.
- Classical TRT applications in cases of high groundwater flow are probably not appropriate to provide the required level of conceptual understanding of a site, both in terms of effective thermal conductivity measured, and identifying where flow is concentrated.
- In cases where temperature changes are not that significant, careful calibration of the FO-DTS is required before any measurements are taken, to ensure good quality data with sufficient signal to noise.

## CRediT authorship contribution statement

**Katerina Kyrkou:** Writing – review & editing, Writing – original draft, Validation, Methodology, Formal analysis, Data curation, Conceptualization. **Joseph Kelly:** Writing – review & editing, Writing – original draft, Methodology, Formal analysis, Data curation, Conceptualization. **Adam Booth:** Writing – review & editing, Writing – original draft, Validation, Methodology, Funding acquisition, Formal analysis, Data curation, Conceptualization. **Fleur Loveridge:** Writing – review & editing, Writing – original draft, Validation, Methodology, Funding acquisition, Formal analysis, Data curation, Conceptualization. **David Boon:** Writing – review & editing, Resources, Formal analysis, Data curation. **Edward Hough:** Writing – review & editing, Resources, Formal analysis, Data curation. **Lawrence Scott:** Writing – review & editing, Resources. **Matthew Jackson:** Writing – review & editing, Writing – original draft, Methodology, Funding acquisition, Conceptualization. **Adrian Butler:** Writing – review & editing, Writing – original draft, Methodology, Funding acquisition, Conceptualization. **Daniel Perez:** Writing – review & editing, Resources. **Athena Chalari:** Resources.

## Declaration of competing interest

The authors declare that they have no known competing financial interests or personal relationships that could have appeared to influence the work reported in this paper.

## Acknowledgments

This work was part of SmartRes ("Smart Assessment, management and optimisation of urban geothermal resources"), a NERC funded collaborative research project between Imperial College London (NE/X005607/1), the British Geological Survey (NE/X005097/1), the University of Leeds (NE/X005496/1) and the University of Manchester (NE/X005135/1). Joseph Kelly is funded by an EPSRC DTP studentship. Laboratory thermal conductivity testing was undertaken by Akshay Nair, under supervision of Jo Thompson, using core plugs, equipment and lab space supplied by the National Geological Repository at the British Geological Survey. Mihai Cimpoiasu, Adrian White, Jason Ngui, Carl Horabin and James Sorensen (British Geological Survey) assisted with U-loop and cable deployment into PL10B. Edward Hough and David Boon publish with the permission of the Executive Director, British Geological Survey. The research team are extremely grateful for access, support and assistance provided by the landowner (Eling Estate) and tenant (Trumpletts Farming) at the site, and the Environment Agency for access to their adjacent compound.

## Data availability

Data will be made available on request.

## References

Ahmed, A.A., Assadi, M., Kalantar, A., Sliwa, T., Sapińska-Śliwa, A., 2022. A critical review on the use of shallow geothermal energy systems for heating and cooling purposes. Energies 15 (12), 4281.

ANSI/CSA C448 SERIES-16 - design and installation of ground source heat pump systems for commercial and residential buildings, 2016.

Bahlali, M., Jacquemyn, C., Jackson, M., Butler, A., Kelly, J., Loveridge, F., Boon, D., Ngui, Y.J., Kuras, O., Chambers, J., Kyrkou, K., Booth, A., 2025. Numerical modelling of highly instrumented thermal response and thermal tracer tests in the UK chalk aquifer. In: European Geothermal Congress 2025, paper 20.

Bloomfield, J., Butler, A.P., Cobbing, J.E., Gallagher, A., Griffiths, K., Moreau, M., Williams, A.T., Peach, D.W., Binley, A., 2003. Flow heterogeneity in the fractured chalk aquifer of southern England. In: *Proceedings of the International Conference on Groundwater in Fractured Rocks*, pp. 29–30. Prague, Czech Republic.

Boon, D.P., Farr, G.J., Hough, E., 2021. "Thermal properties of triassic sherwood (Bunter) sandstone group and mercia mudstone group (Keuper Marl) lithologies". In: 2nd Geoscience & Engineering in Energy Transition Conference, 2021. European Association of Geoscientists & Engineers, pp. 1–5.

Butler, A.P., Mathias, S.A., Gallagher, A.J., Peach, D.W., Williams, A.T., 2009. Analysis of flow processes in fractured chalk under pumped and ambient conditions (UK). Hydrogeol. J. 17 (8), 1849–1858.

Claesson, J., Eskilson, P., 1988. Conductive heat extraction to a deep borehole: thermal analysis and dimensioning rules. Energy 13, 509–527.

Dincer, I., Acar, C., 2015. A review on clean energy solutions for better sustainability. Int. J. Energy Res. 39 (5), 585–606.
Eskilson, P., Hellström, G., Wånggren, B., 1987. Response test for a heat store with 25 boreholes. In: Eskilson, P. (Ed.), Department of Building Technology and Mathematical Physics, Lund Institute of Technology, Sweden, Notes on Heat Transfer 9. Thermal analysis of heat extraction boreholes, Grahns Boktryckeri AB, Lund, Sweden, pp. 130–153 auth.
Fujii, H., Okubo, H., Itoi, R., 2006. Thermal response tests using optical fiber thermometers, 30, pp. 545–551.
Hartog, A., Gamble, G., 1991. Photonic distributed sensing. Phys. World 4, 45–50.
Hoffmann, R., Goderniaux, P., Jamin, P., Orban, P., Brouyère, S., Dassargues, A., 2023. Differentiated influence of the double porosity of the chalk on solute and heat transport. Geol. Soc. London Special Public. 517 (1), 379–387. https://doi.org/10.1144/SP517-2020-170.
Hurtig, E., Großwig, S., Jobmann, M., Kühn, K., Marschall, P., 1994. Fibre-optic temperature measurements in shallow boreholes: experimental application for fluid logging. Geothermics 23 (4), 355–364.
Jackson, M.D., Butler, A.P., Vinogradov, J., 2012. Measurements of spontaneous potential in chalk with application to aquifer characterization in the southern UK. Q. J. Eng. Geol. Hydrogeol. 45 (4), 457–471.
Lord, J.A., Clayton, C.R.I., Mortimore, R.N., 2002. *Engineering in chalk* (Report C574). Construction Industry Research and Information Association (CIRIA).
Loveridge, F., Low, J., Powrie, W., 2017. Site investigation for energy geostructures. Q. J. Eng. Geol. Hydrogeol. 50 (2), 158–168.
Loveridge, F., Holmes, G., Powrie, W., Roberts, T., 2013. Thermal response testing through the chalk aquifer in London, UK. In: Proceedings of the Institution of Civil Engineers-Geotechnical Engineering, 166, pp. 197–210.
MacDonald, A.M., Allen, D.J., 2001. Aquifer properties of the chalk of England. Q. J. Eng. Geol. Hydrogeol. 34, 371–384.
Mathias, S.A., Butler, A.P., Peach, D.W., Williams, A.T., 2007. Recovering tracer test input functions from fluid electrical conductivity logging in fractured porous rocks. Water Resour. Res. 43 (7), W07443. https://doi.org/10.1029/2006WR005455.
Mogensen, P., 1983. Fluid to duct wall heat transfer in duct system heat storages. In: Proceedings of the International Conference on Subsurface Heat Storage in Theory and Practice, Stockholm, 1983. Swedish Council for Building Research, pp. 652–657.
Nair, A.M., 2023. Thermal conductivity of chalk rock in United Kingdom. MSc "Geotechnical Engineering" Dissertation. School of Civil Engineering, University of Leeds.
Parker, S.J., Butler, A.P., Jackson, C.R., 2016. Seasonal and interannual behaviour of groundwater catchment boundaries in a chalk aquifer. Hydrol. Process 30 (1), 3–11.
Price, M., 1987. Fluid flow in the chalk of England. In: goFF, J.C., WilliaMs, B.P.J. (Eds.), Fluid Flow in Sedimentary Basins and Aquifers. Geological Society, Fluid Flow in Sedimentary Basins and Aquifers. Geological Society, 34. Special Publications, London, pp. 141–156.
Price, M., Downing, R.A., Edmunds, W.M., 1993. The chalk as an aquifer. In: Downing, R. A., Price, M., Jones, G.P. (Eds.), *The Hydrogeology of the Chalk of North-West Europe*. Clarendon Press, pp. 35–58.
Raymond, J., Therrien, R., Gosselin, L., Lefebvre, R., 2011. A review of thermal response test analysis using pumping test concepts. Groundwater 49 (6), 932–945.
Rees, S.J., 2016. An introduction to ground-source heat pump technology. Advances in Ground-Source Heat Pump Systems. In: Rees, S.J. (Ed.), *Advances in Ground-Source Heat Pump Systems*. Woodhead Publishing, pp. 1–25. https://doi.org/10.1016/B978-0-08-100311-4.00001-7.
Selker, J.S., Thevenaz, L., Huwald, H., Mallet, A., Luxemburg, W., Van De Giesen, N., Stejskal, M., Zeman, J., Westhoff, M., Parlange, M.B., 2006. Distributed fibre-optic temperature sensing for hydrologic systems. Water Resour. Res. 42 (12).
Signorelli, S., Bassetti, S., Pahud, D., Kohl, T., 2007. Numerical evaluation of thermal response tests. Geothermics 36 (2), 141–166.
Soga, K., 2025. From geo-monitor to geo-adapt: leveraging distributed sensing and data analytics for performance-based design, construction, and maintenance, british geotechnical association rankine lectured, delivered 19th March 2025. Available at: https://www.youtube.com/watch?v=5AxzE7RSGJk.
Spitler, J., Gehlin, S., 2015. Thermal response testing for ground source heat pump systems – an historical review. Renew. Sustain. Energy Rev. 50, 1125–1137.
Vieira, A., Alberdi-Pagola, M., Christodoulides, P., Javed, S., Loveridge, F., Nguyen, F., Cecinato, F., Maranha, J., Florides, G., Prodan, I., Van Lysebetten, G., 2017. Characterisation of ground thermal and thermo-mechanical behaviour for shallow geothermal energy applications. Energies 10 (12), 2044.
Wilke, S., Menberg, K., Steger, H., Blum, P., 2020. Advanced thermal response tests: a review. Renew. Sustain. Energy Rev. 119, 109575.
Williams, A., Bloomfield, J., Griffiths, K., Butler, A., 2006. Characterising the vertical variations in hydraulic conductivity within the chalk aquifer. J. Hydrol. 330 (1–2), 53–62.
Woods, M.A., 2003. Stratigraphy and Correlation of the Chalk Group Seen in the Berkshire Downs LOCAR boreholes(Internal Report IR/03/035). British Geological Survey.
Worthington, S.R.H., Foley, A.E., 2023. In: Farrell, R.P., Massei, N., Foley, A.E., Howlett, P.R., West, L.J. (Eds.), The Chalk Aquifers of Northern Europe, 517. Geological Society, London, pp. 269–283. https://doi.org/10.1144/SP517-2022-111.